

# SCIENTIFIC REPORTS

OPEN

## *In vivo* targeted single-nucleotide editing in zebrafish

Shingo Tanaka<sup>1</sup>, Shin Yoshioka<sup>2</sup>, Keiji Nishida<sup>2</sup>, Hiroshi Hosokawa<sup>3</sup>, Akira Kakizuka<sup>1</sup> & Shingo Maegawa<sup>3</sup>

To date, several genome editing technologies have been developed and are widely utilized in many fields of biology. Most of these technologies, if not all, use nucleases to create DNA double-strand breaks (DSBs), raising the potential risk of cell death and/or oncogenic transformation. The risks hinder their therapeutic applications in humans. Here, we show that *in vivo* targeted single-nucleotide editing in zebrafish, a vertebrate model organism, can be successfully accomplished with the Target-AID system, which involves deamination of a targeted cytidine to create a nucleotide substitution from cytosine to thymine after replication. Application of the system to two zebrafish genes, *chordin* (*chd*) and *one-eyed pinhead* (*oep*), successfully introduced premature stop codons (TAG or TAA) in the targeted genomic loci. The modifications were heritable and faithfully produced phenocopies of well-known homozygous mutants of each gene. These results demonstrate for the first time that the Target-AID system can create heritable nucleotide substitutions *in vivo* in a programmable manner, in vertebrates, namely zebrafish.

Genome editing technologies such as ZFN<sup>1</sup>, TALEN<sup>2</sup> and the CRISPR/Cas9 system<sup>3</sup> have become powerful tools for studying gene functions in model organisms, with a potential for gene therapy in humans<sup>4</sup>. Experimentally, therapeutic genome editing has been achieved in recent studies using technologies that involve non-homologous end joining (NHEJ)-mediated gene disruption<sup>5–8</sup>, NHEJ-mediated gene correction<sup>9</sup>, homology directed repair (HDR)-mediated gene correction<sup>10–12</sup>, and HDR-mediated gene addition<sup>13</sup>. These genome editing technologies have enormous potential for gene therapy. It should be kept in mind, however, that all of these technologies use nucleases to create DNA double-strand breaks (DSBs), and thus carry the risk of cell death and/or oncogenic transformation<sup>14,15</sup>. Therefore, DSB-free genome editing methods should be developed for therapeutic genome editing in humans.

We have recently created a novel single-nucleotide-editing technology that utilizes the CRISPR/Cas9 system for targeting without DSBs<sup>16</sup>. This technology is called the “Target-AID system”. In this system, a fusion protein consisting of nuclease-dead Cas9 (dCas9) or Cas9 nickase (nCas9(D10A))<sup>3</sup>, and the activation-induced cytidine deaminase (AID)<sup>17</sup> derived from sea lamprey, PmCDA1, is introduced in cells with a single guide RNA (sgRNA). The sgRNA recruits the fusion protein, dCas9-PmCDA1, to target sites. AID tethered to dCas9 or nCas9(D10A) can deaminate cytosine in DNA within a five nucleotide window, resulting in the conversion of cytosine to thymine (C > T) after replication. The Target-AID system has been used to generate targeted C > T transitions in *Saccharomyces cerevisiae* and mammalian cultured cells<sup>16</sup>, but not yet in any vertebrates *in vivo*. This system has the potential to allow DSB-free genome editing in vertebrates, including humans, and might provide an alternative approach for gene therapy through single-nucleotide substitutions without DSBs.

Here we describe *in vivo* targeted single-nucleotide editing in zebrafish with the Target-AID system. The *chordin* (*chd*) and *one-eyed pinhead* (*oep*) genes were selected as target genes because the phenotypes induced by the loss (–/–) of each gene are well known. We first showed that the Target-AID system using dCas9-PmCDA1 or nCas9(D10A)-PmCDA1 induced targeted C > T substitutions in zebrafish embryos. Genomic analyses of F<sub>1</sub> embryos produced by the founder fish (G<sub>0</sub> fish), which had been co-injected with the dCas9-PmCDA1 mRNA and sgRNA, revealed that the targeted cytosines were substituted by thymines at appreciable frequencies. In addition, F<sub>2</sub> fish with homozygous nucleotide substitutions in the target genes (*chd* or *oep*) manifested well-known mutant phenotypes. These results demonstrate for the first time that the Target-AID system produces programmable nucleotide substitutions in vertebrates *in vivo*.

<sup>1</sup>Department of Functional Biology, Graduate School of Biostudies, Kyoto University, Kyoto, 606-8501, Japan.

<sup>2</sup>Graduate School of Science, Technology and Innovation, Kobe University, Kobe, Hyogo, 657-8501, Japan. <sup>3</sup>Department of Intelligence Science and Technology, Graduate School of Informatics, Kyoto University, Kyoto, 606-8501, Japan. Correspondence and requests for materials should be addressed to S.M. (email: [shingo@i.kyoto-u.ac.jp](mailto:shingo@i.kyoto-u.ac.jp))



A *chd* gene

		-22	-21	-20	-19	-18	-17	-16	-15	-14	-13	-12	-11	-10	-9	-8	-7	-6	-5	-4	-3	-2	-1			
<b>on-target</b>	Indel	C	A	G	C	A	G	A	G	G	A	G	C	C	G	G	C	G	A	G	G	A	A	G		
uninjected	0																									
dCas9-PmCDA1	0.91				T 2.19																					
nCas9-PmCDA1	8.48				T 4.37										A 0.54 T 0.67	A 0.54	A 0.54		C 0.54	T 0.54						
<b>off-target#1</b>	Indel	G	G	C	G	A	G	A	G	T	A	G	C	C	G	G	C	G	A	G	G	G	A	A	G	
uninjected	0																									
dCas9-PmCDA1	0																									
nCas9-PmCDA1	0																									
<b>off-target#2</b>	Indel	G	C	G	A	T	G	A	G	G	A	G	C	T	G	G	C	G	A	G	G	G	A	C	A	G
uninjected	0																									
dCas9-PmCDA1	0																									
nCas9-PmCDA1	0																									
<b>off-target#3</b>	Indel	G	A	A	C	G	G	A	G	A	C	A	C	C	G	G	C	G	A	G	G	G	A	C	G	G
uninjected	0											G 99.89	T 99.89													
dCas9-PmCDA1	0											G 99.90	T 99.92													
nCas9-PmCDA1	0											G 99.91	T 99.91													

B *oep* gene

		-22	-21	-20	-19	-18	-17	-16	-15	-14	-13	-12	-11	-10	-9	-8	-7	-6	-5	-4	-3	-2	-1			
<b>on-target</b>	Indel	C	A	A	C	G	T	C	A	A	C	A	G	C	G	C	A	A	C	G	C	C	G	A	G	G
uninjected	0																									
dCas9-PmCDA1	0.60				T 2.27			T 1.91																		
nCas9-PmCDA1	1.17				T 1.04																					
<b>off-target#1</b>	Indel	G	G	C	G	G	T	C	T	C	C	G	C	A	G	C	A	A	C	G	C	C	G	C	A	G
uninjected	0																									
dCas9-PmCDA1	0																									
nCas9-PmCDA1	0																									
<b>off-target#2</b>	Indel	T	C	C	C	C	T	C	A	T	T	A	C	C	G	C	C	A	C	G	C	C	G	G	G	G
uninjected	0																									
dCas9-PmCDA1	0																									
nCas9-PmCDA1	0																									

**Figure 2.** The Target-AID system can induce nucleotide substitutions at the target site in injected embryos. DNA sequences aligned in a row represent the reference sequences of target and off-target regions (DanRer10). The targeting sequences, mismatched bases, and PAM sequences in the DNA sequences are highlighted in gray, light blue, and yellow, respectively. Mutational frequencies (%) at each nucleotide position (-22 to -1) from the PAM sequences are shown below the DNA sequences. (A) A mutation spectrum in the *chd* locus obtained by deep sequencing for uninjected embryos, dCas9-PmCDA1 mRNA-injected embryos, and nCas9-PmCDA1 mRNA-injected embryos. (B) A mutation spectrum in the *oep* locus obtained by deep sequencing for uninjected embryos, dCas9-PmCDA1 mRNA-injected embryos, and nCas9-PmCDA1 mRNA-injected embryos. On average, more than 90,000 reads were obtained per sample.

previously reported<sup>16</sup>. With respect to the *chd* sgRNA, we analyzed three potential off-target sites. These potential off-target sites have 1- to 4-base mismatches from the true target site. Deep sequencing revealed that off-target#1 and off-target#2 contained no mutations in the uninjected embryos, none in dCas9-PmCDA1 mRNA-injected embryos, and none in nCas9-PmCDA1 mRNA-injected embryos (Fig. 2A). Off-target#3 had A > G and C > T substitutions at two positions (-10 and -12), both with almost 100% frequencies, which were most likely due to pre-existing single nucleotide polymorphisms rather than induced substitutions (Fig. 2A).

Next, we evaluated the *oep* gene locus (Fig. 2B). In each experiment, we analyzed sixteen embryos injected with *oep* sgRNA and dCas9-PmCDA1 mRNA, or sixteen embryos injected with *oep* sgRNA and nCas9-PmCDA1 mRNA, by deep sequencing. Collectively, as expected, targeted C > T substitutions were observed in the dCas9-PmCDA1 mRNA-injected embryos (2.27% at the -19 position (c.175 C), and 1.91% at the -16 position (c.178 C)). In the nCas9-PmCDA1 mRNA-injected embryos, targeted C > T substitutions were detected only at the -19 position (1.04%). Indel mutations were detected approximately 2 times less frequently in the dCas9-PmCDA1 mRNA-injected embryos (0.60%) than in the nCas9-PmCDA1 mRNA-injected embryos (1.17%). Similar to what we observed in the *chd* locus, HMA assays revealed that dCas9-PmCDA1 induced fewer indel mutations in the *oep* locus than nCas9-PmCDA1 and Cas9 (Suppl. Fig. 1D–F). Thus, the Target-AID system can induce targeted C > T substitutions with few indels in the *oep* gene locus in zebrafish embryos.

We next examined off-target effects in the *oep* locus. For the *oep* sgRNA, we analyzed two potential off-target sites. The potential off-target sites predicted by CCTop contained 4-base mismatches from the true target site. Deep sequencing revealed that both the potential off-target sites contained no mutations in the uninjected embryos, none in the dCas9-PmCDA1 mRNA-injected embryos, and none in the nCas9-PmCDA1 mRNA-injected embryos (Fig. 2B).

In summary, both constructs, dCas9-PmCDA1 and nCas9-PmCDA1, were able to induce targeted C > T substitutions in zebrafish embryos without apparent off-target effects, at least in the putative off-target sites. In particular, dCas9-PmCDA1 induced targeted C > T substitutions in both loci with fewer indel mutations than nCas9-PmCDA1 in zebrafish embryos. Importantly, the ratio of base substitutions to indel mutations<sup>20</sup> with dCas9-PmCDA1 was higher than that with nCas9-PmCDA1 (in the *chd* locus, 2.41 for dCas9-PmCDA1 and 0.52 for nCas9-PmCDA1; and in the *oep* locus, 3.78 for dCas9-PmCDA1 and 0.97 for nCas9-PmCDA1). We therefore chose dCas9-PmCDA1 for the following experiments.

**Generation of G<sub>0</sub> adult zebrafish carrying the expected nucleotide substitutions.** We injected dCas9-PmCDA1 mRNA with the *chd* sgRNA or *oep* sgRNA into zebrafish embryos to generate G<sub>0</sub> adult zebrafish (Suppl. Fig. 2). The adult fish are referred to as *chd* G<sub>0</sub> fish or *oep* G<sub>0</sub> fish, respectively. To investigate whether the G<sub>0</sub> fish had the expected nucleotide substitutions at the target sites, PCR amplification of the targeted sequences

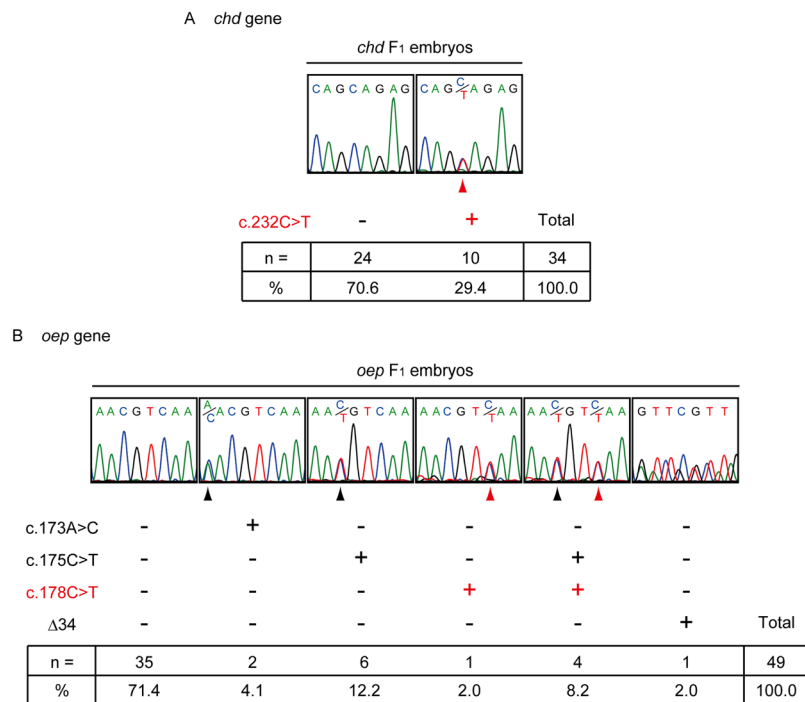


**Figure 3.** The nucleotide substitutions induced by the Target-AID system are heritable. Sequence patterns of (A) *chd* F<sub>1</sub> embryos and (B) *oep* F<sub>1</sub> embryos. The red arrowheads indicate nucleotide substitutions at the target site. The black arrowheads indicate nucleotide substitutions at untargeted sites. Observed frequencies and percentages of each genotype are shown in the panel.

was performed using genomic DNA from the caudal fins of five male *chd* G<sub>0</sub> fish, and the PCR fragments were sequenced. Nucleotide substitutions were detected as extra peaks below the major peaks, likely due to mosaicism of the G<sub>0</sub> fish (black and red arrowheads in Suppl. Fig. 3). In the analyses of *chd* G<sub>0</sub> fish, two sequence patterns were obtained. One pattern, seen in three *chd* G<sub>0</sub> fish, contained no detectable change (pattern (i) in Suppl. Fig. 3A); in the other pattern, two *chd* G<sub>0</sub> fish had nucleotide substitutions at the target site, c.232 C (pattern (ii) in Suppl. Fig. 3A). No deletions were found around the target nucleotides in the *chd* gene. There were no detectable changes in non-targeted cytosines in the adjacent region around the target site in all analyzed *chd* G<sub>0</sub> fish.

In the analyses of five male *oep* G<sub>0</sub> fish, one fish had no detectable changes (pattern (i) in Suppl. Fig. 3B), and among the other fish, three types of nucleotide substitutions were observed (pattern (ii) to (v) in Suppl. Fig. 3B). The first type had a c.175 C > T substitution (black arrowheads in Suppl. Fig. 3B). The second type had a c.178 C > T substitution (red arrowheads in Suppl. Fig. 3B). In the third type, both c.175 C > T and c.178 C > T substitutions were present. Pattern (v), seen in one *oep* G<sub>0</sub> fish, likely arose from mosaicism involving the expected nucleotide substitution of c.175 C and c.178 C, as well as at least one small deletion (Suppl. Fig. 3B). According to the experimental design, we expected that c.175 C and c.178 C, but no other nucleotide, would be mutated. Indeed, there were no detectable changes at other cytosines in the adjacent region around the target site in all analyzed *oep* G<sub>0</sub> fish.

**The induced nucleotide substitutions were mostly heritable in the next generation.** In order to examine whether the nucleotide substitutions induced by the Target-AID system in the G<sub>0</sub> fish were heritable, genotyping of descendant embryos of the G<sub>0</sub> fish was performed. Wild-type females were bred with the *chd* G<sub>0</sub> fish or *oep* G<sub>0</sub> fish (Suppl. Fig. 2), and descendant embryos were obtained from three *chd* G<sub>0</sub> fish and four *oep* G<sub>0</sub> fish (*chd* F<sub>1</sub> embryos and *oep* F<sub>1</sub> embryos, respectively). We then performed PCR amplification of the targeted sequences using genomic DNA from F<sub>1</sub> embryos and sequenced the PCR products. Nucleotide substitutions were detected as superimposed peaks because the F<sub>1</sub> embryos were mostly heterozygous at the target loci (black and red arrowheads in Fig. 3).

Analysis of the genomic DNA from *chd* F<sub>1</sub> embryos revealed two patterns in the *chd* loci (Fig. 3A). Expected c.232 C > T nucleotide substitutions were detected with a frequency of 29.4% (10/34). No detectable change was observed in the rest of the *chd* F<sub>1</sub> embryos, 70.6% (24/34). Moreover, no other nucleotide substitutions were found within the sequenced regions. Germ line transmission of the modified allele was achieved in two of the three *chd* G<sub>0</sub> fish (Suppl. Table 1).

From the analyses of *oep* F<sub>1</sub> embryos from four *oep* G<sub>0</sub> fish, we observed six patterns of sequence results (Fig. 3B): 1) 71.4% (35/49) of *oep* F<sub>1</sub> embryos did not contain nucleotide changes; 2) 2.0% (1/49) contained a c.178 C > T substitution; 3) 12.2% (6/49) contained c.175 C > T substitutions; 4) 8.2% (4/49) contained both c.175 C > T and c.178 C > T substitutions; and 5) 2.0% (1/49) contained a deletion, detected in one sequencing result. Unexpectedly, in a sixth pattern two *oep* F<sub>1</sub> embryos had a c.173 A > C substitution at a frequency of 4.1%

(2/49). Three of the four *oep* G<sub>0</sub> fish successfully transmitted the modified alleles (Suppl. Table 2). Note that one *oep* G<sub>0</sub> fish with both the c.175 C > T and c.178 C > T substitutions (pattern (iv) in Fig. 3B) produced only wild-type F<sub>1</sub> embryos (Fig. 3B and Suppl. Table 2). Taken together, these results indicate that the nucleotide substitutions induced by the Target-AID system are heritable.

We next raised the rest of the F<sub>1</sub> embryos to adulthood (Suppl. Fig. 2) and performed allele-specific PCR (Fig. 4A–C, E–G) and sequencing (Fig. 4D, H) to identify heterozygous F<sub>1</sub> fish carrying the desired nucleotide substitutions at the target sites. For the identification of promising candidate heterozygous *chd* F<sub>1</sub> fish carrying the c.232 C > T substitution (*chd*<sup>c.232C>T/+</sup>), we performed two PCR reactions using allele-specific primers, one for the wild-type allele (w) and the other for the mutated allele (m). Both produced 203 bp fragments (Fig. 4B, C). Another set of primers, which was designed to amplify the *chd* gene outside of the target site, was also included in the PCR reaction. This produced 635 bp DNA fragments as internal positive controls (Fig. 4B, C). When the 203 bp DNA fragment was detected only in a “w” lane, the result indicated that the fish did not carry the c.232 C > T substitution, and the fish was scored as a “negative” or “wild-type” fish (*chd*<sup>+/+</sup> fish). If the 203 bp DNA fragments were detected in both “w” and “m” lanes, the fish was heterozygous, and was scored as “positive” or “mutated” (*chd*<sup>c.232C>T/+</sup> fish). In total, we identified 39 “negative” (*chd*<sup>+/+</sup>) and 12 “positive” (*chd*<sup>c.232C>T/+</sup>) fish (Fig. 4C). Sequencing of the targeted region in the 12 positive fish confirmed the c.232 C > T substitution in all 12 fish (Fig. 4D).

We next examined *oep* F<sub>1</sub> fish to identify candidate heterozygotes carrying the C > T nucleotide substitution (*oep*<sup>c.178C>T/+</sup> fish) (Fig. 4E–G). For this purpose, we used sets of allele-specific primers for the wild-type allele (w) or for the mutated allele (m) (183 bp fragments in Fig. 4E, G), and another set of control primers (415 bp fragments in Fig. 4E, G), and performed allele-specific PCR. We found 147 (*oep*<sup>+/+</sup>) and 16 (*oep*<sup>c.178C>T/+</sup>) fish (Fig. 4G). Sequencing of the targeted region in the 16 (*oep*<sup>c.178C>T/+</sup>) fish revealed that 12 fish were compound heterozygotes with c.175 C > T and c.178 C > T substitutions, and 4 were heterozygotes for the c.178 C > T substitution only (Fig. 4H).

### The nucleotide substitutions at target cytosines recapitulate typical mutant phenotypes.

Next, we bred a pair of *chd*<sup>c.232C>T/+</sup> fish or a pair of *oep*<sup>c.178C>T/+</sup> fish to produce F<sub>2</sub> embryos (Suppl. Fig. 2). As described above, the c.232 C > T and c.178 C > T nucleotide substitutions in the *chd* and *oep* genes, respectively, create premature stop codons (Fig. 1). Thus, the F<sub>2</sub> embryos with homozygous mutations should display well-known phenotypes: *chd* mutants have small heads and expanded blood islands<sup>21</sup>, and *oep* mutants have single eyes<sup>22</sup>. The breeding experiments revealed that typical *chd* mutant and *oep* mutant phenotypes were observed in 28.4% (61/215) and 21.6% (68/315) of the F<sub>2</sub> embryos, respectively. These results fit well with a recessive mode of Mendelian inheritance. Sequence analyses of the genomes of these embryos revealed the expected genotypes, namely F<sub>2</sub> embryos with small heads and expanded blood islands were *chd*<sup>c.232C>T/c.232C>T</sup> homozygotes (Fig. 5B compared with 5A), and F<sub>2</sub> embryos with single eyes were *oep*<sup>c.178C>T/c.178C>T</sup> homozygotes (Fig. 5D, F, compared with 5C, E, respectively).

To further characterize *oep*<sup>c.178C>T/c.178C>T</sup> F<sub>2</sub> embryos, we performed whole mount *in situ* hybridizations with RNA probes for *gooseoid* (*gsc*), a molecular marker for the organizer, and *hatching gland 1* (*hgg1*), a molecular marker for anterior dorsal mesoderm (Fig. 5G–J). The expression of *gsc* was suppressed at the shield stage in *oep*<sup>c.178C>T/c.178C>T</sup> embryos (Fig. 5H compared with 5G). This observation was consistent with a previous study<sup>22</sup>. Moreover, the expression of *hgg1* was absent at the tailbud stage in *oep*<sup>c.178C>T/c.178C>T</sup> embryos (Fig. 5J compared with 5I). These observations are also consistent with previously described phenotypes of *oep* mutants<sup>22</sup>, demonstrating that *oep*<sup>c.178C>T/c.178C>T</sup> embryos recapitulate mesodermal defects characteristic of *oep* mutant embryos. These results, as a whole, convincingly show that the Target-AID system can introduce a targeted single-nucleotide substitution from cytosine to thymine *in vivo* in a vertebrate.

### Discussion

It has been shown that the Target-AID system<sup>16</sup> and another nucleotide editing system<sup>20</sup> deliver single-nucleotide alterations in *Saccharomyces cerevisiae* and mammalian cultured cells. The Target-AID system is based on the CRISPR/Cas9 system<sup>16</sup> which functions as a powerful tool for gene knockouts in various kinds of vertebrates, such as medaka<sup>18</sup>, *Xenopus*<sup>23,24</sup>, and mouse<sup>25,26</sup> as well as invertebrates<sup>27,28</sup>. Therefore, programmable single-nucleotide editing of genomic DNA in these various organisms should be amenable to the Target-AID system. Indeed, we show in this study that the Target-AID system can induce heritable nucleotide substitutions in zebrafish *in vivo*.

We evaluated two versions of the Target-AID system, dCas9-PmCDA1 and nCas9-PmCDA1, in zebrafish embryos. In a previous study of the Target-AID system, formation of nicks on the non-deamination strand of target DNA appeared to improve the frequency of C > T substitutions at the target sites<sup>16</sup>. Deep sequencing in injected embryos in the present study revealed that DNA nicking by nCas9-PmCDA1 improved the frequency of targeted C > T substitutions in the *chd* locus in zebrafish embryos, but not in the *oep* locus. Moreover, nCas9-PmCDA1 induced C > A, G > T, G > C, or G > A substitutions in addition to C > T substitutions in the *chd* locus, and increased indel mutations to a level that we consider problematic (Fig. 2 and Suppl. Fig. 1). In fact, indel mutations in zebrafish were observed in another nCas9-based base editing (BE) method, which induced C > T substitutions<sup>29</sup>. In sharp contrast, we observed efficient targeted C > T substitutions and hardly observed indel mutations with dCas9-PmCDA1, as compared to nCas9-PmCDA1. These results suggest that the Target-AID system using dCas9-PmCDA1 provides a safer single-nucleotide-editing method, as compared to nCas9-PmCDA1, for therapeutic applications in animals.

Deep sequencing of G<sub>0</sub> embryos and analyses of F<sub>1</sub> embryos revealed that the nucleotide substitutions at the target sites occurred with different frequencies. These differences may be dependent on the distances from the PAM sequences. With the *chd* gene, dCas9-PmCDA1 yielded the c.232 C > T mutation at the -19 position from

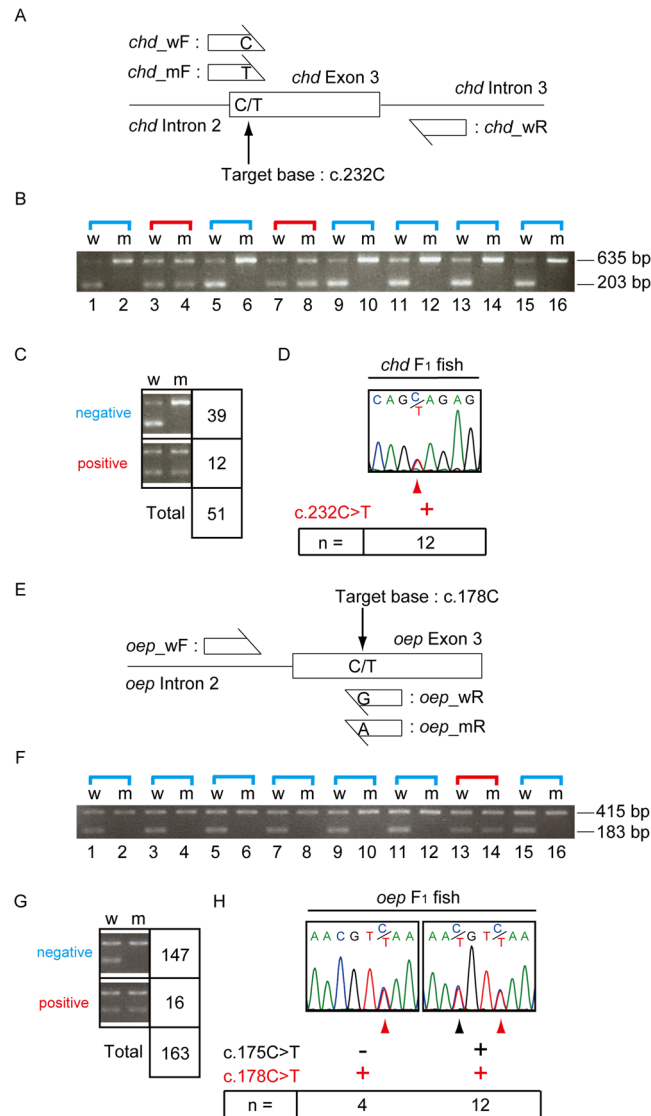


**Figure 4.** Identification of heterozygous fish carrying the expected nucleotide substitution at the target site. **(A)** Schematic representation of allele-specific PCR analysis of the *chd* gene. **(B)** An example of the results after allele-specific PCR amplification of the *chd* gene. The 203 bp DNA fragments in the “w” lanes were amplified by the primer set of *chd\_wF* and *chd\_wR* primers, whereas fragments in the “m” lanes were amplified by the primer set of *chd\_mF* and *chd\_wR*. The 635 bp DNA fragments were amplified by a primer set recognizing a different region of the *chd* gene as an internal control. **(C)** Results of analyzing all individuals by allele-specific PCR for the *chd* gene. “Negative” indicates the absence of a nucleotide substitution at the target site, while “positive” indicates the presence of a nucleotide substitution at the target site. **(D)** Results of analyzing 12 positive individuals by sequencing the targeted region of the *chd* gene. **(E)** Schematic representation of allele-specific PCR analysis for the *oep* gene. **(F)** An example of results after allele-specific PCR amplification of the *oep* gene. The 183 bp DNA fragments in the “w” lanes were amplified by the primer set *oep\_wF* and *oep\_wR*, whereas fragments in the “m” lanes were amplified by the primer set *oep\_wF* and *oep\_mR*. The 415 bp DNA fragments were amplified by a primer set recognizing a different region of the *oep* gene as an internal control. **(G)** Results of analyzing all individuals by allele-specific PCR for the *oep* gene. **(H)** Results of analyzing 16 positive individuals by sequencing the targeted region of the *oep* gene. **(D,H)** The red arrowheads indicate the nucleotide substitution at the target site. **(H)** The black arrowhead indicates the nucleotide substitution at the untargeted site.

the PAM sequence at a frequency of 2.19% in G<sub>0</sub> embryos (Fig. 2A). With the *oep* gene, the c.175C>T substitution (at position -19 with respect to the PAM) and the c.178C>T substitution (at position -16 with respect to the PAM) were induced by dCas9-PmCDA1 in G<sub>0</sub> embryos at frequencies of 2.27% and 1.91%, respectively (Fig. 2B). In F<sub>1</sub> embryos, the *chd* c.232C>T mutation was obtained at an overall frequency of 29.4% (10/34), and this was the sole mutation that was obtained (Fig. 3A). The c.175C>T substitution was present in 20.4% of the *oep* F<sub>1</sub> embryos, and the c.178C>T substitution was present in 10.2% of the *oep* F<sub>1</sub> embryos (Fig. 3B) when including compound heterozygotes with both -19 and -16 substitutions. These frequencies, in particular in F<sub>1</sub> embryos, were reminiscent of those observed in a Target-AID system, using nCas9(D10A)-PmCDA1 in yeast<sup>16</sup>;

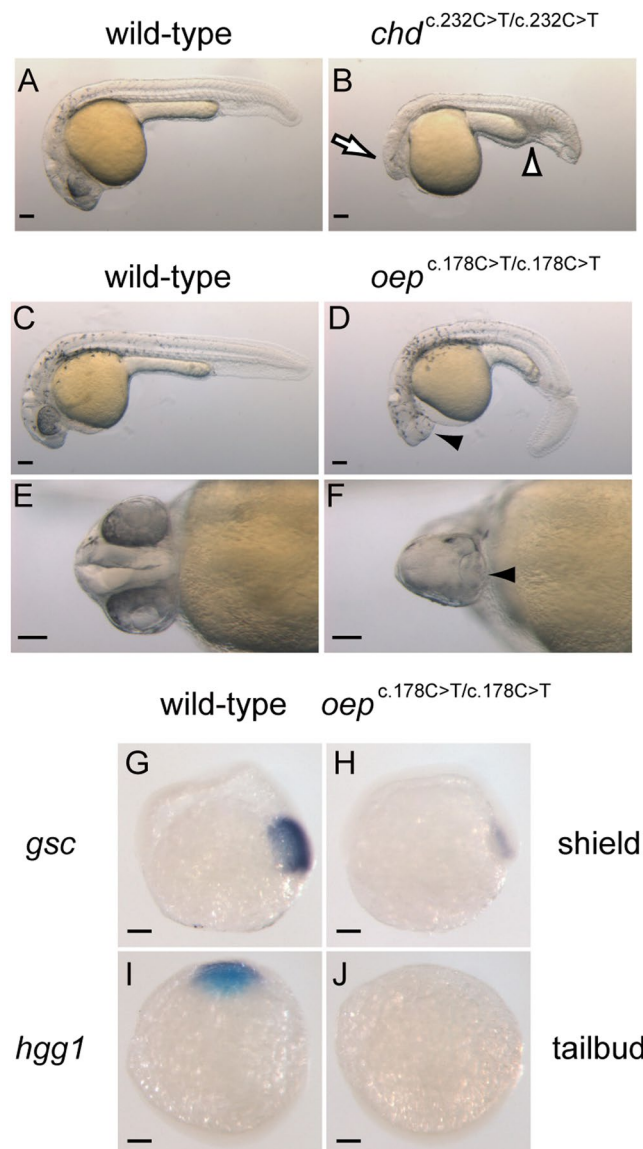


**Figure 5.** The Target-AID system can generate nucleotide substitution mutants. Phenotypic representation of (A, lateral view) a wild-type embryo and (B, lateral view) a *chd*<sup>c.232C>T/c.232C>T</sup> F<sub>2</sub> embryo at 24 hpf. The open arrow and open arrowhead indicate a smaller head and expanded blood islands, respectively. Phenotypic representation of (C, lateral view), (E, ventral view) a wild-type embryo and (D, lateral view), (F, ventral view) an *oep*<sup>c.178C>T/c.178C>T</sup> F<sub>2</sub> embryo at 27 hpf. The arrowhead indicates a single eye in each respective panel. (G,H) Expression pattern of *gsc* in (G, lateral view) a wild-type embryo and (H, lateral view) an *oep*<sup>c.178C>T/c.178C>T</sup> F<sub>2</sub> embryo at the shield stage. (I,J) Expression pattern of *hgg1* in (I, dorsal view) a wild-type embryo and (J, dorsal view) an *oep*<sup>c.178C>T/c.178C>T</sup> F<sub>2</sub> embryo at the tailbud stage. Scale bars represent 100 μm.

with the yeast system, nucleotide substitutions of cytosines occurred at the -19 position at a frequency of about 25%, and substitutions at the -16 position occurred with a frequency of about 5%. Our results suggest that, even in zebrafish, the relative distance from the PAM affects the efficiency of cytidine deamination. Our results also indicate that candidate regions for targeted mutations should ideally have only one cytosine, in order to avoid redundant modifications.

Interestingly, base substitution rates in germ lines were higher than those of whole embryos in deep sequencing (Fig. 3A,B compared with Fig. 2A,B). Our observation suggests that base substitutions by dCas9-PmCDA1 might occur more effectively in germline cells than in somatic cells.

We also found A > C substitutions in the *oep* F<sub>1</sub> embryos (Fig. 3B). The previous study reported that the A > C substitutions induced by the Target-AID system are rare (less than 1%)<sup>16</sup>. A deaminated adenine (hypoxanthine) is capable of base pairing with cytosine in *E. coli*, resulting in an A > G mutation<sup>30</sup>. However, this mechanism cannot explain the A > C substitution that we observed in the present study. A deletion event was also observed, even though nuclease-dead Cas9 was used for targeting (Figs 2, 3B, Suppl. Figs 1, and 3B). Deletion events with the Target-AID system using dCas9-PmCDA1 were also detected in the previous study at a frequency of less than

1%<sup>16</sup>. This deletion might be due to the sequence context in the targeted region and/or epigenetic modifications of the target loci. Further studies are needed for a detailed understanding of the rare A > C substitutions and deletions induced by the Target-AID system.

Off-target assessments in G<sub>0</sub> embryos revealed that the Target-AID system did not appear to create off-target mutations, at least in the putative off-target sites we examined (Fig. 2). These results indicate that strict base-pair matching is required for the induction of C > T substitutions in zebrafish. Of course, there is a slight possibility that some of the injected embryos might die by 3 dpf because of unpredictable off-target effects. Further analysis about off-target effects of the Target-AID system is required to more precisely evaluate the Target-AID system *in vivo*.

G<sub>0</sub> fish whose caudal fins possessed the desired nucleotide substitutions did not always transmit the nucleotide substitutions to their F<sub>1</sub> descendants. The results are consistent with the possibility of mosaicism, where different nucleotide substitutions occurred in each daughter cell after the cell division of the zygote co-injected with the dCas9-PmCDA1 mRNA and sgRNA. The results also indicate that the genotype of cells in caudal fins is not a perfect indicator of germline transmission.

In addition to the creation of premature stop codons, as shown in this study, the Target-AID system has a potential to regulate transcription and splicing *in vivo*. It is difficult to make suitable precise modifications at promoter/enhancer regions or splicing sites by the regular CRISPR/Cas9 system because the CRISPR/Cas9 system induces uncontrolled DSBs. In contrast, the Target-AID system may allow researchers to modulate the promoter/enhancer activities and splicing pattern/efficiency by the substitutions of appropriate target cytosines with thymines in the promoter/enhancer and splicing sites, respectively. In this regard, the Target-AID system may provide an opportunity for therapeutic treatment by regulating gene expression and/or splicing. Future efforts will be directed toward overcoming the limitation of the PAM recognition, etc., to achieve nucleotide substitutions at any desired position of the genome.

## Methods

**Zebrafish.** Zebrafish were maintained as described in a previous study<sup>31</sup>. Wild-type embryos were obtained by breeding AB strain males and females. All zebrafish experiments were performed under the ethical guidelines of Kyoto University and approved by the Animal Experimentation Committee of Kyoto University (No. Inf-K14001).

**mRNA synthesis.** The DNA coding sequences for dCas9-NLS-FLAG-PmCDA1 (dCas9-PmCDA1), and nCas9-NLS-FLAG-PmCDA1 (nCas9-PmCDA1) were amplified by PCR with the following primer set: 5'-TCTTTTTCAGGATCATGGACAAGAAGTAC-3', and 5'-GAGAGGCCTTGAATTGGATCCTTATCCGGA-3'. The PCR products were cloned into the pCS2+ vector using the InFusion method (Takara, Kusatsu, Japan). The resulting pCS2+ dCas9-PmCDA1, the pCS2+ nCas9-PmCDA1, and the pCS2+ Cas9 plasmid was linearized with NotI. Capped mRNA encoding dCas9-PmCDA1, nCas9-PmCDA1, and Cas9 was synthesized *in vitro* from the SP6 promoter using a mMESAGE mMACHINE SP6 kit (Thermo Fisher Scientific, Waltham, USA) following the manufacturer's protocol.

**Single guide RNA synthesis.** For synthesis of sgRNAs with customizable 18-nucleotide targeting sequences, we used the oligonucleotide pairs listed in Suppl. Table 3. Each oligonucleotide pair was annealed at 25 °C for 1 h after incubation at 95 °C for 2 min. The annealed oligonucleotides were ligated into BsaI-digested pDR274 vector<sup>18,32</sup> with Ligation high Ver.2 (Toyobo, Osaka, Japan). After the ligated products were linearized with DraI, sgRNAs were synthesized *in vitro* using MEGashortscript T7 Transcription Kit (Thermo Fisher Scientific, Waltham, USA) according to the manufacturer's protocol.

**RNA injection.** Approximately 1 nl of the following mixed solutions was microinjected into the cytoplasm of 1-cell stage zebrafish embryos: dCas9-PmCDA1 mRNA + *chd* sgRNA (100 ng/μl dCas9-PmCDA1 mRNA, 25 ng/μl *chd* sgRNA); nCas9-PmCDA1 mRNA + *chd* sgRNA (100 ng/μl nCas9-PmCDA1 mRNA, 25 ng/μl *chd* sgRNA); Cas9 mRNA + *chd* sgRNA (100 ng/μl Cas9 mRNA, 25 ng/μl *chd* sgRNA); dCas9-PmCDA1 mRNA + *oep* sgRNA (100 ng/μl dCas9-PmCDA1 mRNA, 25 ng/μl *oep* sgRNA); nCas9-PmCDA1 mRNA + *oep* sgRNA (100 ng/μl nCas9-PmCDA1 mRNA, 25 ng/μl *oep* sgRNA); and Cas9 mRNA + *oep* sgRNA (100 ng/μl Cas9 mRNA, 25 ng/μl *oep* sgRNA). For the *chd* sgRNA, on average, 96.6% of uninjected embryos, 77.8% of dCas9-PmCDA1 mRNA-injected embryos, 76.4% of nCas9-PmCDA1 mRNA-injected embryos, and 61.4% of Cas9 mRNA-injected embryos showed apparently normal phenotypes at 3 dpf. For the *oep* sgRNA, on average, 95.2% of uninjected embryos, 67.3% of dCas9-PmCDA1 mRNA-injected embryos, 57.6% of nCas9-PmCDA1 mRNA-injected embryos, and 47.2% of Cas9 mRNA-injected embryos showed apparently normal phenotypes at 3 dpf. Injected embryos with apparently normal phenotypes were used for deep sequencing and the heteroduplex mobility assays described below.

**Fin amputation.** Adult zebrafish were anesthetized in 0.6 mM Tricaine solution (Sigma-Aldrich, St Louis, USA). Zebrafish caudal fins were amputated with a surgical blade (No. 10, FEATHER Safety Razor, Mino, Japan).

**Genomic DNA preparation.** For genomic DNA preparation, amputated caudal fins of adult fish or whole single embryos at 1–3 dpf were lysed essentially as described<sup>18</sup>. The lysates were used for PCR amplification.

**Deep sequencing of target and off-target sites in zebrafish embryos.** Genomic DNA, extracted from each zebrafish embryo at 3 dpf, was used as template DNA for primary PCR amplification. Deep sequencing

was carried out as previously described<sup>16</sup>. The primers used for deep sequencing are listed in Suppl. Table 3. After nested PCR, index sequences were added to the amplicons. The index sequences were matched to samples as described in Suppl. Table 4. Sequencing reactions were performed with a MiniSeq sequencing system (Illumina, CA, USA) to obtain paired 151 bp read lengths. The obtained reads were mapped to each reference sequence from the zebrafish genome database (DanRer10) by the following setting: Masking mode = no masking; Mismatch cost = 2; Insertion cost = 3; Deletion cost = 3; Length fraction = 0.5; Similarity fraction = 0.8; Global alignment = No; Auto detect paired distances = Yes; Nonspecific match handling = Map randomly. The variant calling was performed with the following settings: Ignore positions with coverage = 150,000; Ignore broken pairs = Yes; Ignore Nonspecific matches = Reads; Minimum coverage = 10; Minimum count = 2; Minimum frequency = 0.5%; Base quality filter = No; Read detection filter = No; Relative read direction filter = 0.5%; Read position filter = No; Remove pyro-error variants = No. Rearrangement of the output file was made using Excel (Microsoft, WA, USA).

**Heteroduplex mobility assay.** Heteroduplex mobility assays (HMA) were performed essentially as described in a previous study<sup>18</sup>. Targeting sequences in the *chd* and *oep* loci were amplified with BIOTAQ DNA Polymerase (Bioline, London, UK) and with primer sets listed in Suppl. Table 3. The primer sets produce 117 bp DNA fragments for the *chd* locus, and 132 bp DNA fragments for the *oep* locus. The DNA fragments were separated by electrophoresis in an 8.0% acrylamide gel.

**Genotyping by sequencing.** PCR amplification of the targeting sequences in the *chd* and *oep* genes was performed with BIOTAQ DNA Polymerase (Bioline, London, UK) and with primer sets listed in Suppl. Table 3. PCR was carried out with the following parameters: for the *chd* gene, a pre-denaturation of 94 °C for 5 min, 30 cycles of amplification (94 °C for 20 s, 62 °C for 20 s and 72 °C for 20 s), and a final extension at 72 °C for 1 min; for the *oep* gene, a pre-denaturation of 94 °C for 5 min, 30 cycles of amplification (94 °C for 20 s, 55 °C for 20 s and 72 °C for 20 s), and a final extension at 72 °C for 1 min. The PCR products from the *chd* and *oep* amplifications were purified with NucleoSpin Gel and PCR Clean-up (Macherey-Nagel, Düren, Germany) and sequenced by Fasmac (Atsugi, Japan) or by MacroGen Japan (Kyoto, Japan) with the *chd*\_1st\_F and *oep*\_1st\_F primers, respectively.

**Genotyping by allele-specific PCR.** Primers used in allele-specific PCR<sup>33</sup> are listed in Suppl. Table 3. The *chd*\_wF and the *chd*\_mF primers were designed to anneal to the antisense strand of intron 2 and exon 3 in the *chd* gene, while the *chd*\_wR primer to the sense strand of intron 3 in the *chd* gene. The 3' ends of both of the forward primers were designed to anneal to the target nucleotide, c.232 C, in the *chd* gene. The *chd*\_wF primer has a C residue at the 3' end, while the *chd*\_mF primer has a T residue at the 3' end. Moreover, a T residue two nucleotides from the 3' ends of both of the forward primers generates a template/primer C/T mismatch. The *oep*\_wF primer was designed to anneal to the antisense strand of intron 2 in the *oep* gene, while the *oep*\_wR and *oep*\_mR primers to the sense strand of exon 3 in the *oep* gene. The 3' ends of both of the reverse primers were designed to anneal to the target nucleotide, c.178 C, in the *oep* gene. The *oep*\_wR primer has a G residue at the 3' end, while the *oep*\_mR primer has an A residue at the 3' end. The primer sets of *chd*\_bF and *chd*\_bR, and *oep*\_bF and *oep*\_bR were used for internal controls to amplify DNA sequences 800–1400 bp downstream of the target nucleotides.

Allele-specific PCR for the target nucleotides in the *chd* and *oep* genes was performed with BIOTAQ DNA Polymerase (Bioline, London, UK) with the following PCR parameters: for the *chd* gene, a pre-denaturation of 94 °C for 5 min, 30 cycles of amplification (94 °C for 20 s, 60 °C for 20 s and 72 °C for 20 s) and a final extension at 72 °C for 1 min; for the *oep* gene, a pre-denaturation of 94 °C for 5 min, 25 cycles of amplification (94 °C for 20 s, 55 °C for 20 s and 72 °C for 20 s) and a final extension at 72 °C for 1 min. The PCR products were separated by electrophoresis in a 2.0% agarose gel.

**Phenotypic observation of zebrafish embryos.** The phenotypes of F<sub>2</sub> embryos were observed at 24 hours post fertilization (hpf) for the *chd* mutant embryos and at 27 hpf for the *oep* mutant embryos. Images of the embryos were taken under a SZX16 stereo microscope (Olympus, Tokyo, Japan) equipped with a MicroPublisher 5.0 camera (QImaging, Surrey, Canada).

**Whole mount *in situ* hybridization.** Each RNA probe was synthesized to detect *gsc*, or *hgg1* endogenous mRNA, as described previously<sup>34</sup>. Whole mount *in situ* hybridization was performed by a protocol described previously<sup>35</sup>. Genomic DNA from each embryo was extracted essentially as described<sup>36</sup>. The genotype of each embryo was determined by allele-specific PCR.

**Data availability.** Data obtained by deep sequencing have been deposited in the NCBI Sequence Read Archive (SRA), and the accession code is SRP140583. The remaining data are available from the corresponding author upon request.

## References

- Kim, Y. G., Cha, J. & Chandrasegaran, S. Hybrid restriction enzymes: Zinc finger fusions to Fok I cleavage domain. *Proceedings of the National Academy of Sciences of the United States of America* **93**, 1156–1160, <https://doi.org/10.1073/pnas.93.3.1156> (1996).
- Christian, M. *et al.* Targeting DNA Double-Strand Breaks with TAL Effector Nucleases. *Genetics* **186**, 757–U476, <https://doi.org/10.1534/genetics.110.120717> (2010).
- Jinek, M. *et al.* A Programmable Dual-RNA-Guided DNA Endonuclease in Adaptive Bacterial Immunity. *Science* **337**, 816–821, <https://doi.org/10.1126/science.1225829> (2012).
- Cox, D. B. T., Platt, R. J. & Zhang, F. Therapeutic genome editing: prospects and challenges. *Nature Medicine* **21**, 121–131 (2015).
- Ding, Q. R. *et al.* Permanent Alteration of PCSK9 With *In Vivo* CRISPR-Cas9 Genome Editing. *Circulation Research* **115**, 488–+, <https://doi.org/10.1161/circresaha.115.304351> (2014).

6. Lin, S. R. *et al.* The CRISPR/Cas9 System Facilitates Clearance of the Intrahepatic HBV Templates *In Vivo*. *Molecular Therapy-Nucleic Acids* **3** <https://doi.org/10.1038/mtna.2014.38> (2014).
7. Tebas, P. *et al.* Gene Editing of CCR5 in Autologous CD4 T Cells of Persons Infected with HIV. *New England Journal of Medicine* **370**, 901–910, <https://doi.org/10.1056/NEJMoa1300662> (2014).
8. Bakondi, B. *et al.* *In Vivo* CRISPR/Cas9 Gene Editing Corrects Retinal Dystrophy in the S334ter-3 Rat Model of Autosomal Dominant Retinitis Pigmentosa. *Molecular Therapy* **24**, 556–563, <https://doi.org/10.1038/mt.2015.220> (2016).
9. Nelson, C. E. *et al.* *In vivo* genome editing improves muscle function in a mouse model of Duchenne muscular dystrophy. *Science* **351**, 403–407, <https://doi.org/10.1126/science.aad5143> (2016).
10. Schwank, G. *et al.* Functional Repair of CFTR by CRISPR/Cas9 in Intestinal Stem Cell Organoids of Cystic Fibrosis Patients. *Cell Stem Cell* **13**, 653–658, <https://doi.org/10.1016/j.stem.2013.11.002> (2013).
11. Wu, Y. X. *et al.* Correction of a Genetic Disease in Mouse via Use of CRISPR-Cas9. *Cell Stem Cell* **13**, 659–662, <https://doi.org/10.1016/j.stem.2013.10.016> (2013).
12. Long, C. Z. *et al.* Prevention of muscular dystrophy in mice by CRISPR/Cas9-mediated editing of germline DNA. *Science* **345**, 1184–1188, <https://doi.org/10.1126/science.1254445> (2014).
13. De Ravin, S. S. *et al.* Targeted gene addition in human CD34(+) hematopoietic cells for correction of X-linked chronic granulomatous disease. *Nature Biotechnology* **34**, 424–+, <https://doi.org/10.1038/nbt.3513> (2016).
14. Rich, T., Allen, R. L. & Wyllie, A. H. Defying death after DNA damage. *Nature* **407**, 777–783 (2000).
15. Nambiar, M. & Raghavan, S. C. How does DNA break during chromosomal translocations? *Nucleic Acids Research* **39**, 5813–5825, <https://doi.org/10.1093/nar/gkr223> (2011).
16. Nishida, K. *et al.* Targeted nucleotide editing using hybrid prokaryotic and vertebrate adaptive immune systems. *Science* **353**, 1248–+, <https://doi.org/10.1126/science.aaf8729> (2016).
17. Muramatsu, M. *et al.* Specific expression of activation-induced cytidine deaminase (AID), a novel member of the RNA-editing deaminase family in germinal center B cells. *Journal of Biological Chemistry* **274**, 18470–18476, <https://doi.org/10.1074/jbc.274.26.18470> (1999).
18. Ansai, S. & Kinoshita, M. Targeted mutagenesis using CRISPR/Cas system in medaka. *Biology Open* **3**, 362–371, <https://doi.org/10.1242/bio.20148177> (2014).
19. Stemmer, M., Thumberger, T., Keyer, M. d. S., Wittbrodt, J. & Mateo, J. L. CCTop: An Intuitive, Flexible and Reliable CRISPR/Cas9 Target Prediction Tool. *Plos One* **10** <https://doi.org/10.1371/journal.pone.0124633> (2015).
20. Komor, A. C., Kim, Y. B., Packer, M. S., Zuris, J. A. & Liu, D. R. Programmable editing of a target base in genomic DNA without double-stranded DNA cleavage. *Nature* **533**, 420–+, <https://doi.org/10.1038/nature17946> (2016).
21. Hammerschmidt, M. *et al.* dino and mercedes, two genes regulating dorsal development in the zebrafish embryo. *Development* **123**, 95–102 (1996).
22. Schier, A. F., Neuhauss, S. C. F., Helde, K. A., Talbot, W. S. & Driever, W. The one-eyed pinhead gene functions in mesoderm and endoderm formation in zebrafish and interacts with no tail. *Development* **124**, 327–342 (1997).
23. Blitz, I. L., Biesinger, J., Xie, X. H. & Cho, K. W. Y. Biallelic Genome Modification in F-0 *Xenopus tropicalis* Embryos Using the CRISPR/Cas System. *Genesis* **51**, 827–834, <https://doi.org/10.1002/dvg.22719> (2013).
24. Nakayama, T. *et al.* Simple and Efficient CRISPR/Cas9-Mediated Targeted Mutagenesis in *Xenopus tropicalis*. *Genesis* **51**, 835–843, <https://doi.org/10.1002/dvg.22720> (2013).
25. Shen, B. *et al.* Generation of gene-modified mice via Cas9/RNA-mediated gene targeting. *Cell Research* **23**, 720–723, <https://doi.org/10.1038/cr.2013.46> (2013).
26. Wang, H. Y. *et al.* One-Step Generation of Mice Carrying Mutations in Multiple Genes by CRISPR/Cas-Mediated Genome Engineering. *Cell* **153**, 910–918, <https://doi.org/10.1016/j.cell.2013.04.025> (2013).
27. Friedland, A. E. *et al.* Heritable genome editing in *C. elegans* via a CRISPR-Cas9 system. *Nature Methods* **10**, 741–+, <https://doi.org/10.1038/nmeth.2532> (2013).
28. Gratz, S. J. *et al.* Genome Engineering of *Drosophila* with the CRISPR RNA-Guided Cas9 Nuclease. *Genetics* **194**, 1029–+, <https://doi.org/10.1534/genetics.113.152710> (2013).
29. Zhang, Y. H. *et al.* Programmable base editing of zebrafish genome using a modified CRISPR-Cas9 system. *Nature Communications* **8** <https://doi.org/10.1038/s41467-017-00175-6> (2017).
30. Nordmann, P. L., Makris, J. C. & Reznikoff, W. S. Inosine induced mutations. *Molecular & General Genetics* **214**, 62–67, <https://doi.org/10.1007/bf00340180> (1988).
31. Aoyama, Y. *et al.* A Novel Method for Rearing Zebrafish by Using Freshwater Rotifers (*Brachionus calyciflorus*). *Zebrafish* **12**, 288–295, <https://doi.org/10.1089/zeb.2014.1032> (2015).
32. Hwang, W. Y. *et al.* Efficient genome editing in zebrafish using a CRISPR-Cas system. *Nature Biotechnology* **31**, 227–229, <https://doi.org/10.1038/nbt.2501> (2013).
33. Newton, C. R. *et al.* Analysis of any point mutation in DNA - The amplification refractory mutation system (ARMS). *Nucleic Acids Research* **17**, 2503–2516, <https://doi.org/10.1093/nar/17.7.2503> (1989).
34. Maegawa, S., Varga, M. & Weinberg, E. S. FGF signaling is required for beta-catenin-mediated induction of the zebrafish organizer. *Development* **133**, 3265–3276, <https://doi.org/10.1242/dev.02483> (2006).
35. Tanaka, S., Hosokawa, H., Weinberg, E. S. & Maegawa, S. Chordin and dickkopf-1b are essential for the formation of head structures through activation of the FGF signaling pathway in zebrafish. *Developmental biology* **424**, 189–197, <https://doi.org/10.1016/j.ydbio.2017.02.018> (2017).
36. Gansner, J. M., Madsen, E. C., Mecham, R. P. & Gitlin, J. D. Essential Role for fibrillin-2 in Zebrafish Notochord and Vascular Morphogenesis. *Developmental Dynamics* **237**, 2844–2861, <https://doi.org/10.1002/dvdy.21705> (2008).

## Acknowledgements

We thank Dr. Kinoshita for kindly providing the pCS2+ Cas9 vector. We also thank our lab members for maintaining our fish facility. S.M. was supported by a Grant-in-aid for Young Scientists (A) No. 22687016 and for Exploratory Research No. 24657102. This work was partly supported by the New Energy and Industrial Technology Development Organization (NEDO).

## Author Contributions

S.T., S.M., K.N. and H.H. designed the research and S.T., S.Y. and S.M. carried out the experiments. S.T., S.M., H.H. and A.K. wrote the manuscript. All authors analyzed and discussed the results.

## Additional Information

**Supplementary information** accompanies this paper at <https://doi.org/10.1038/s41598-018-29794-9>.

**Competing Interests:** The authors declare no competing interests.

**Publisher's note:** Springer Nature remains neutral with regard to jurisdictional claims in published maps and institutional affiliations.



**Open Access** This article is licensed under a Creative Commons Attribution 4.0 International License, which permits use, sharing, adaptation, distribution and reproduction in any medium or format, as long as you give appropriate credit to the original author(s) and the source, provide a link to the Creative Commons license, and indicate if changes were made. The images or other third party material in this article are included in the article's Creative Commons license, unless indicated otherwise in a credit line to the material. If material is not included in the article's Creative Commons license and your intended use is not permitted by statutory regulation or exceeds the permitted use, you will need to obtain permission directly from the copyright holder. To view a copy of this license, visit <http://creativecommons.org/licenses/by/4.0/>.

© The Author(s) 2018